Available online at www.sciencedirect.com

SciVerse ScienceDirect

Physics Procedia 41 (2013) 713 – 722

Physics Procedia

Lasers in Manufacturing Conference 2013

All fiber laser scribing of Cu(In,Ga)Se_2 thin-film solar modules

A. Burn[a]*, M. Muralt[a], S. Pilz[a], V. Romano[a], R. Witte[b], B. Frei[b], S. Buecheler[c], S. Nishiwaki[c], L. Krainer[d]

[a]*Bern University of Applied Sciences, Pestalozzistrasse 20, CH-3400 Burgdorf, +41 34 426 4141*
[b]*Solneva SA, Swiss Solar Tools, Alte Lyssstrasse 2, CH-3270 Aarberg, +41 31 588 2500*
[c]*Laboratory for Thin Films and Photovoltaics, EMPA, Swiss Federal Laboratories for Materials Science and Technology, Überlandstrasse 129, CH-8600 Dübendorf, +41 44 823 5511*
[d]*Onefive GmbH, In Böden 139, CH-8046 Zürich, +41 43 538 36 57*

Abstract

State-of-the-art Cu(In,Ga)Se2 thin-film technology allows the industrial production of highly efficient solar modules. A significant growth of CIGS-based solar cell production volume can be expected for the coming years. One of the critical manufacturing steps in module production is thin-film patterning which allows the monolithic integration of cell-to-cell interconnects. Today, solar module manufacturers seek to replace sub-optimal needle scribing by suitable laser processes. It has been demonstrated, that ultra-short pulse laser scribing can reduce the overall width per interconnect and increase scribe quality. A promising tool for picosecond laser-scribing is the fiber laser. Here we present the successful implementation of all fiber laser patterning of CIGS modules.

Keywords: CIGS; thin-film patterning; laser scribing; picosecond processing; fiber laser; selective ablation

1. Introduction

Simple up-scaling of the surface of a single thin-film solar cell would result in high current densities in the transparent electrical front contact which causes considerable Ohmic losses in the cell. High efficiency on large solar modules can be achieved by dividing the cell area into strips (or sub-cells) that are connected in

* Corresponding author. Tel.: +41-34-426-4246
E-mail address: andreas.burn@bfh.ch.

doi:10.1016/j.phpro.2013.03.138

series. Electrical interconnects between neighboring cells can be built in the thin-film stack (Fig. 1a) without introducing external material just by scribing three individual lines between process steps. Along these scribes the thin films are selectively removed as illustrated in Fig. 1b for a typical scribe arrangement.

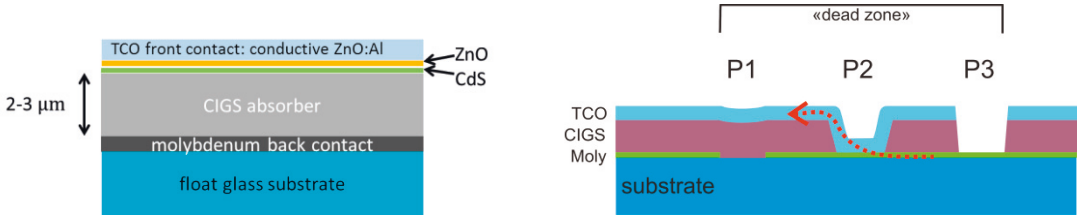

Fig. 1. (a) Anatomy of a Cu(In,Ga)Se_2 thin-film solar cell on glass substrate. (b) Cross-section through an interconnect with the three scribes P1-P3 made between the three main thin-film deposition process steps. The P1 scribe creates an isolating line in the molybdenum-coated sheet glass substrate. Then the CIGS layer is grown on top, followed by the P2 scribe which removes the CIGS and exposes the moly back contact. In the third step, the front contact – a transparent conductive oxide (TCO) layer – is deposited and patterned in the P3 scribing process. Together, the three scribes form an electrical back-to-front contact as indicated by the dashed arrow. The non-productive area covered by the three scribes is termed the "dead zone".

While in today's production lines the P1 process is often a laser process, P2 and P3 are still mechanical needle scribes. Considerable efforts have been made to develop stable and reliable laser processes for P2 and P3 scribing. Various strategies were developed which employed pulsed laser sources with femtosecond to nanosecond pulse durations at different wavelengths. Promising results were reported by for pulse durations in the short picosecond (10-30 ps) and long femtosecond region by Zoppel et al., 2007, Račiukaitis, 2011, Burn et al., 2012, Gecys et al., 2012, Witte et al., 2013 but also nanosecond pulses can lead to stable processes in some cases as reported earlier by Compaan et al., 2000.

In an earlier work (Burn et al., 2012) we conducted an extensive parameter study incorporating many commercially available laser sources in order to identify and characterize stable process windows in different process and pulse length regimes. We identified the pulse duration region around 30 ps as well suited for reliable P1, P2 and P3 scribing. Those processes were found to work stable in a large process window with respect to focal distance and pulse energy. These appealing results were realized with a high-end solid state laser (SSL) which offers decent characteristics such as very good pulse energy stability, high pulse energy, short pulse length and very good beam quality. Laser systems of this class are rather bulky and expensive but most important they are quite heavy. Due to their form factor and mass solid state lasers are not easy to integrate into moving head machine configurations. Long free space beam paths and moving mirrors are generally necessary in such cases. This also means time-consuming and costly alignment and cleaning or sealing of delicate optical elements. However, especially in the thin-film solar industry the moving process head machine concept offers some clear advantages such as a small machine footprint and relatively low inertia of moving parts. Reliable fiber delivery of the laser pulses to the process head can solve these problems and is therefore a key enabler technology for many of these machine concepts. Fiber delivery works well for pulse durations longer than a couple of hundred picoseconds and for multi-mode beams but is not practicable with 30 ps pulses, single-mode in the necessary pulse energy range of 1-10 µJ due to some strong non-linear effects in the fiber which distort the temporal and spatial shape of the pulse and can make it unusable for stable high quality processing.

An interesting alternative became recently available with a new class of all-in-fiber lasers such as the Katana HP from onefive GmbH, Switzerland. These lasers have a relatively small, light and mechanically stable laser head which can be mounted on fast moving axes. The head is connected to the main supply by only one optical cable which goes into an ordinary cable drag chain along with other electrical connections.

Beside the easier machine integration these lasers can be built smaller, lighter and air-cooled, which goes along with a potentially lower total cost of ownership compared to SSLs. Their disadvantage is the considerably lower maximum pulse energy, longer pulses of typically ≥50 ps and slightly lower beam quality.

In the present study we tried to transfer successful scribing processes realized on solid state lasers to a state-of-the art picosecond all-in-fiber laser platform. The goal is the assessment of the picosecond fiber laser as a tool for industrial all-laser patterning of CIGS thin-film solar modules.

2. Experimental

2.1. Laser sources

We used an all-in-fiber MOPA laser system from onefive GmbH, Switzerland with pulse duration of approximately 50 ps and up to 11 µJ pulse energy at 1064 nm and 5 µJ at 532 nm. The optical system was kept as simple as possible: just a single-element focusing lens with focal length selected to produce a focal spot diameter d_0 of approximately 25 µm.

The solid state laser used in the experiments was a MOPA system from Time-Bandwidth products, Switzerland. The intrinsic pulse duration of the laser is <10 ps but for this application the pulses were stretched to approximately 30 ps using an etalon. The system also offers second and third harmonic output.

2.2. Scribing machine

All fiber laser scribing was done on a two-axis linear motion system (see Fig. 2) with an effective working area of 350 x 950 mm^2. The scribing speed on a 100 x 100 mm^2 sample is typically 1 m/s along the shorter axis and up to 2 m/s along the longer axis. This motion system is made from industrial-grade components

Fig. 2. Scribing machine with optical experimentation platform on top. In the middle of the platform sits the motorized z-axis; here with two separate beam paths for 532 nm and 1064 nm. When the photograph was taken, two laser sources were installed: the box on the left is the head of the picosecond fiber laser with external second harmonic generation (SHG), on the right is the head of a nano-second pulsed fiber laser. The empty space on the right is used for beam diagnostics with a scanning slit beam profiler and other tools.

(linear motors and controller electronics) and was manufactured by Solneva SA. The position repeatability of the whole system on the full effective working area is 1 µm for the shorter axis and 1.8 µm for the longer axis. The scribing machine features a large optical experimentation platform on top which allows fast installation and exchange of laser sources. With this setup new laser sources can be integrated quickly because all equipment needed is a simple focusing element. This works also with exotic wavelengths as there are no scanning mirrors etc. needed. The system is further equipped with a motorized z-axis for adjusting the focal plane position relative to the sample surface. The whole system is computer-controlled via a specifically developed software program which also provides an interface to control the laser source. This solution allows batch processing of full parameter studies with controlled variation of pulse energy, scribing velocity and focal position. It is also possible to write scripts for full P1, P2 or P3 patterning of a functional sample. Finally, a vision system with telecentric optics provides in-situ measurement and inspection capability.

The solid state laser scribing was done with a state-of-the art galvanometric scanning head equipped with an f-theta lens of 160 mm focal length. Module scribe patterns were programmed using professional marking software.

2.3. Functional module fabrication

Scribing experiments were made on latest generation Mo/CIGS/TCO thin film samples grown on 50 x 50 x 1 mm^3 float glass substrates. All thin film samples were produced at the Laboratory for Thin Films and Photovoltaics, EMPA, Dübendorf, Switzerland (Chirila et al., 2011). Several series of functional 8-cell mini modules have been produced for process assessment with selected parameter sets. These functional mini-modules provide excellent process quality feedback as their electrical properties can be tested under standardized conditions. A typical module layout is reproduced in Fig. 3a.

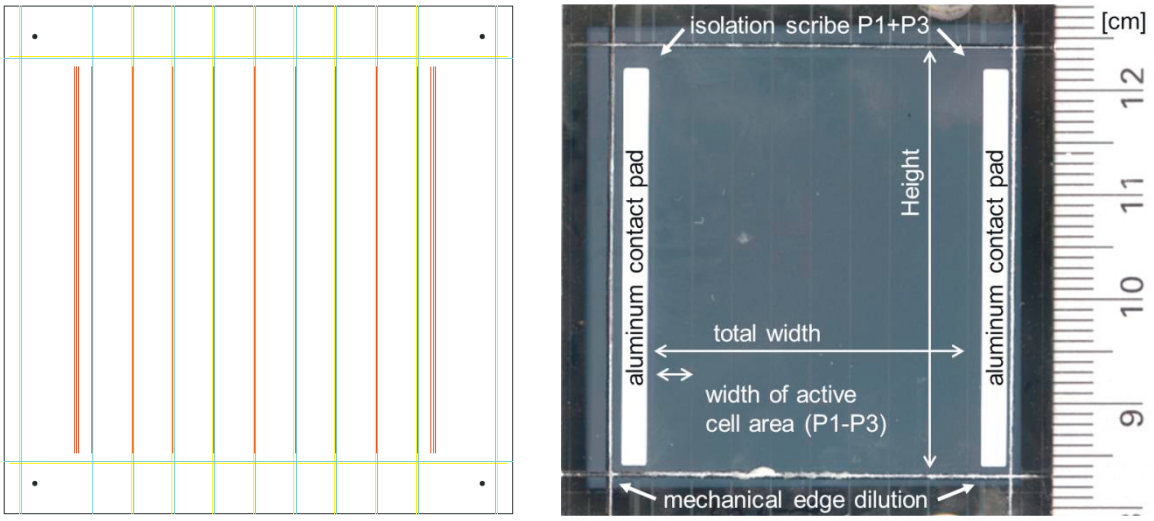

Fig. 3. (a) pattern used for laser scribing of 8-cell mini-modules P1-yellow, P2-red, P3-blue. (b) finished functional module with evaporated aluminum contact bars for electrical testing and additional mechanical edge dilution lines.

Scribing parameters for the functional modules in the solid state laser control group were chosen according to the best parameter sets found in a previous study (Burn et al., 2012). For the fiber laser processes, a small parameter study has been conducted for each of the P1, P2 and P3 processes prior to the structuring of functional modules. This was necessary in order to adapt the processes to the differing characteristics of the

fiber laser (pulse duration, pulse shape, maximum pulse energy) with respect to the solid state laser. The laser parameters chosen for functional module production are presented in Tab. 1. Parameters for P1 at a wavelength of 532 nm and 1064 nm were found to lead to equally good results in previous experiments. Parameter values for 1064 nm and 512 nm are therefore both indicated in Tab. 1. However, functional modules evaluated for this study were all P1-structured at 1064 nm only.

laser system	P1			P2			P3		
	λ	E_p	OL	λ	E_p	OL	λ	E_p	OL
solid-state MOPA	532 nm	4.0 µJ	40 %	532 nm	1.0 µJ	99 %	532 nm	1.0 µJ	30 %
Δτ = 30 ps	1064 nm	6.0 µJ	30 %						
all-in-fiber MOPA	532 nm	4.0 µJ	40 %	532 nm	1.3 µJ	99 %	532 nm	3.0 µJ	30 %
Δτ = 50 ps	1064 nm	9.5 µJ	20 %						

Table 1. Laser parameter sets used for P1-P3 scribing of the functional modules. Beam waist radius ω_0 was 12-16 µm for all processes. Symbols: λ: wavelength, E_p: pulse energy, OL: pulse-to-pulse overlap

2.4. Functional module analysis

Single scribes and finished modules were analyzed for scribe quality and surface topography using optical microscopy, laser scanning microscopy (LSM), model: Zeiss LSM Pascal 5 and scanning electron microscopy (SEM), model: Zeiss Sigma VP. Local material composition and process selectivity was determined using energy-dispersive X-ray spectroscopy (EDX); type: Oxford INCA Energy 350, detector: XMax 80.

Electrical testing of the functional solar modules was done by means of illuminated current voltage (J-V) characteristics at the EMPA laboratory. The J-V measurements were accomplished according to the international standard IEC 60904-1 under standard test conditions with AM1.5G irradiation spectrum and 1000 Wm^{-2} irradiation intensity. The devices under test were kept at constant temperature of 25°C during measurement. The area of the devices was determined from a 1200 dpi scan using graphical software. Typically, the active surface was around 12.56 cm^2 per module and 1.57 cm^2 per cell (8 cells).

Prior to the testing all modules were equipped with evaporated aluminum contact bars and a mechanical edge dilution was applied in order to assure that the module edges are potential-free. This mechanical edge dilution was applied outside the laser isolation scribes as shown in fig. 3b. The designated illumination area is defined solely by the laser isolation scribes.

3. Results

3.1. P1 scribing process

Quality criteria for a good P1 scribe are: good electrical isolation, no delamination at the scribe borders, no burr formation, no cracks and no damage in the substrate. In Fig. 4 the results of both, the all-fiber laser scribe and the SSL scribe are depicted side by side for comparison. Both scribes guarantee a very good electrical isolation of >60MΩ (highest measurable value of Ohm-meter used) for the full scribe length of 40 mm. In both cases the scribe borders show a clean rupture of the molybdenum layer. A detailed inspection of the side-walls of the fiber laser scribe shows that neither delamination, nor burr or cracks (perpendicular to the scribe) are present. The process runs stable with constantly good results in a large process parameter window and even tolerates significant changes in the molybdenum film dimension and quality.

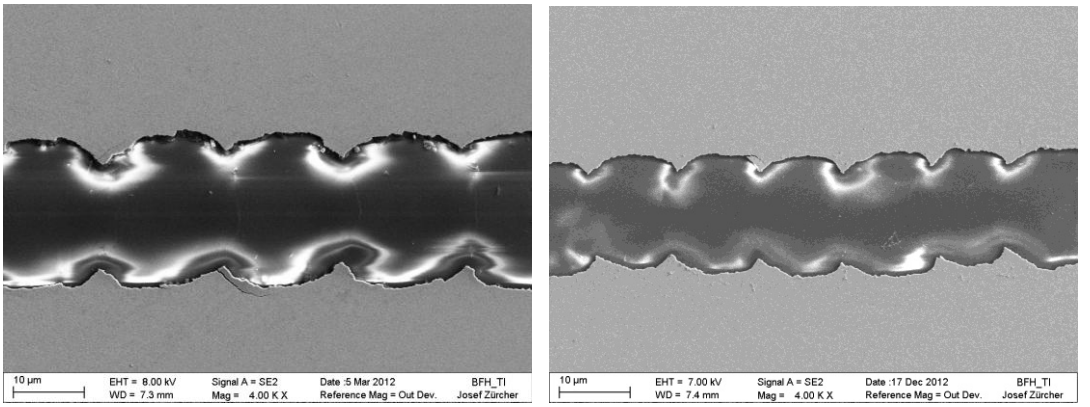

Fig. 4. SEM images of two typical P1 scribe lines (a) SSL, 1064 nm, 30 ps, 6 µJ, overlap 30% (b) fiber laser, 532 nm, 50 ps, 4 µJ, overlap 40%.

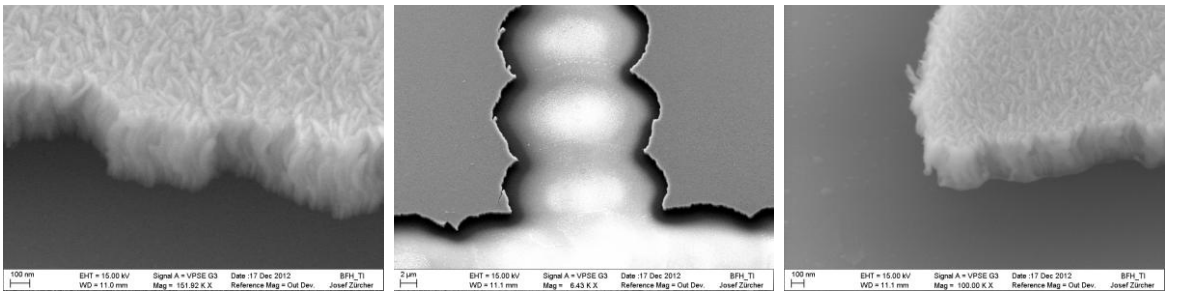

Fig. 5. High magnification electron micrographs made with the variable pressure secondary electron (VPSE) detector in order to reduce charge build-up. Images show a scribe made with the fiber laser at 532 nm. Left: Detail of the scribe border which shows a clean mechanical fracture of the molybdenum layer. Middle: critical crossing of two P1 scribes at the edge of the module. The process outcome is not affected by this special situation. Right: detail of the scribe crossing – no significant melting and no delamination even if three quarters of the neighboring material is removed.

3.2. P2 scribing process

Quality criteria for the P2 scribing process are: Molybdenum back contact integrity, width of the exposed back contact versus width of the molten CIGS zone, height and profile of the burr, cracks and bubbles in the molten CIGS. Another important point is the electrical contact resistance of the exposed back contact which strongly depends on the surface quality. This, however, is not accessible for direct measurements but must be evaluated during electrical testing (it is contained in the series resistance of the module which becomes apparent in its characteristic J-V curve).

Once the approximate parameter values are found the P2 scribing process works equally well with the 50 ps fiber laser as with the 30 ps SSL. Both processes work stable in a quite large pulse energy range and produce high quality results as shown in Fig. 6. The most critical parameter in both cases is the translation speed i.e. the pulse-to-pulse overlap. This value determines scribe border quality and width of the exposed back contact strip.

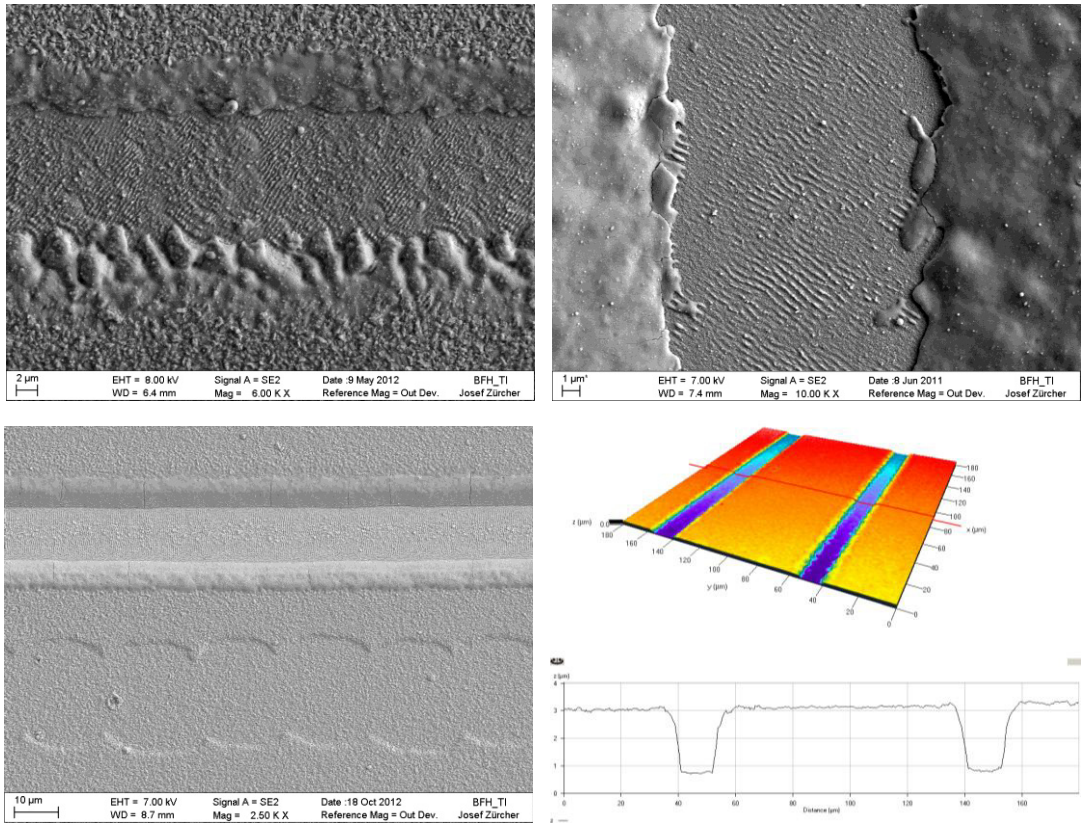

Fig. 6. SEM images of typical P2 scribe lines (top row) SSL, 532 nm, 30 ps, 1 µJ, overlap 99% . (bottom row) fiber laser, 532 nm, 50 ps, 1.3 µJ, overlap 99%. On the left a typical P2 scribe along a covered P1 scribe and on the right a typical LSM height profile of a fiber laser P2 scribe.

3.3. P3 scribing process

Critical for a good P3 scribe is a secure electrical interruption of the TCO front contact. The border of the scribe should be clearly defined and excessive melting and heat affection must be avoided to reduce the possibility of parasitic short formation. A lift-off type process is therefore usually preferred. Historically, the P3 process involves the complete removal of the absorber layer down to the back contact as shown in Fig. 1b. However, we found that removal of just the front TCO layer is sufficient, at least if the following conditions are fulfilled: a) the scribe width is substantially bigger than twice the absorber layer thickness b) there is only a marginal amount of molten absorber material in the scribe c) the pulse duration of the laser is short enough (<1ns) and the pulse-to-pulse overlap is small in order to avoid heat accumulation.

The process itself is highly tolerant against variations in the pulse length and overlap. However, the pulse energy is critical, especially if the pulse energy drops below a certain (local) limit which depends on many local variables like adhesion, thickness and optical transmissivity of the TCO film etc. Using pulse energies slightly higher than absolutely necessary can greatly reduce the risk of electrical shorts due to incomplete TCO removal. The increased melting is not a problem as long as the significant heat accumulation is avoided. In general the presented process is easily controllable and produces excellent results.

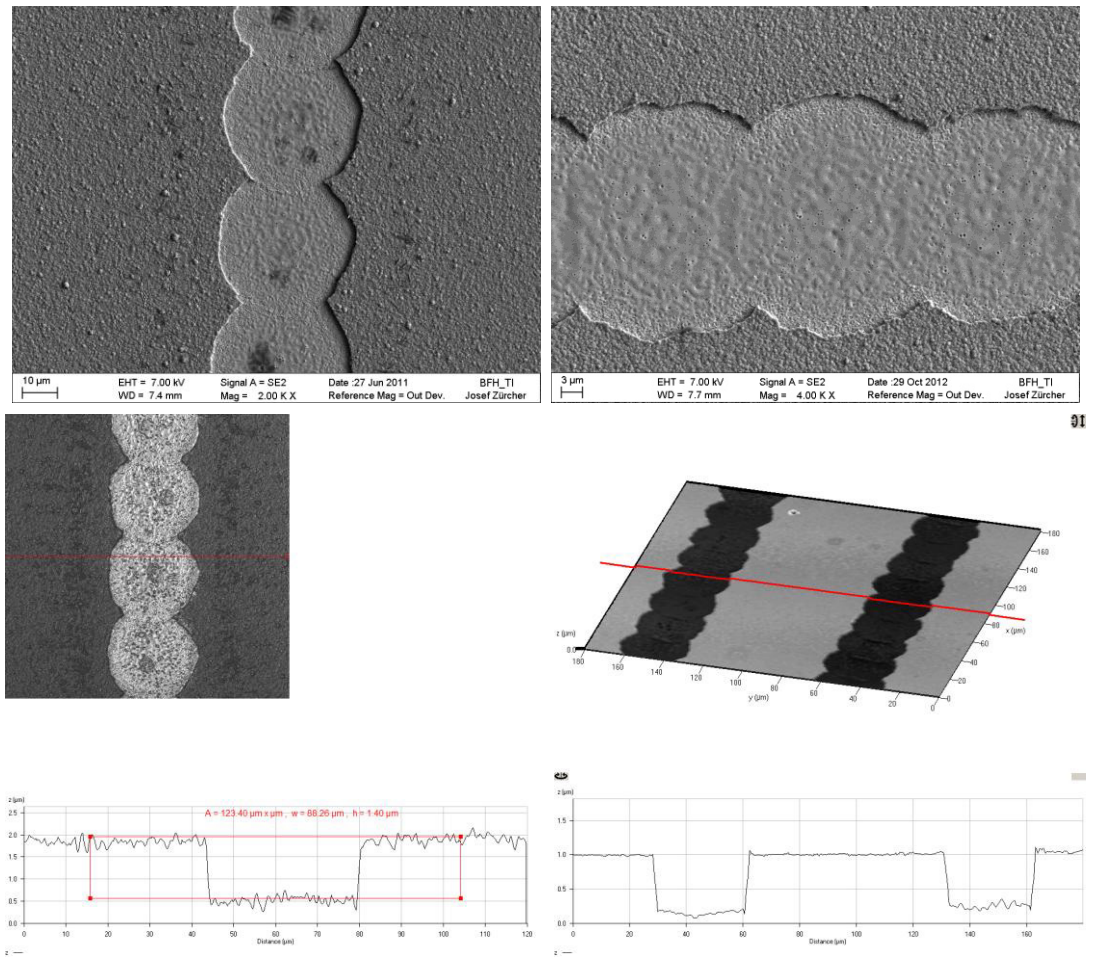

Fig. 7. SEM images of typical P3 scribe lines. (left column) SSL, 532 nm, 30 ps, 2 µJ, overlap 10%. (right column) fiber laser scribe, 532 nm, 50 ps, 4 µJ, overlap 40%. Bottom row: LSM height profiles of the P3 scribes above.

3.4. Functional module performance

A functional module is fabricated mainly for testing the electrical performance of the module as a system consisting of active PV thin films, laser scribing processes and their geometric arrangement on the sample. Often, after an extensive process study the fabrication of a functional module also brings a significant enlargement of the statistics as the total scribe length increases dramatically compared to short test scribes made during the process study. In the present case where the transfer of known processes to a new class of lasers is the overall goal, the optical inspection of the results is also important as it can already reveal some fundamental differences in the process outcome. SEM images of a typical section of both the SSL fabricated sample and the fiber-laser one are presented in Fig. 8. Optically the two interconnects look very similar with only a slight change in the P2 scribe border profile.

The reduced dead zone width of the fiber-laser structured sample is due to the different scribing setup used. The scribes on the left image were made using galvanometric scanners and since 1064 nm and 532 nm were used, also two scanners with two different f-theta lenses were necessary. The limiting factors of galvo scanners for dead-zone reduction in PV thin-film scribing are often linearity-deviations and barrel- and pin-cushion distortions, especially if the optics is exchanged between processes. The scribing machine which was used together with the fiber-laser does not show this type of distortion. Together with the good repeatability a drastic reduction in dead-zone width can be achieved which goes even beyond the situation in Fig. 8, right image. Not to forget: a 125 µm dead-zone is already 3-4 times smaller than the industrial needle scribe standard.

The selectivity of the laser processes has been investigated using EDX and a similar approach as described by Burn et al., 2012 with comparable results. Scribes on both modules showed good process selectivity.

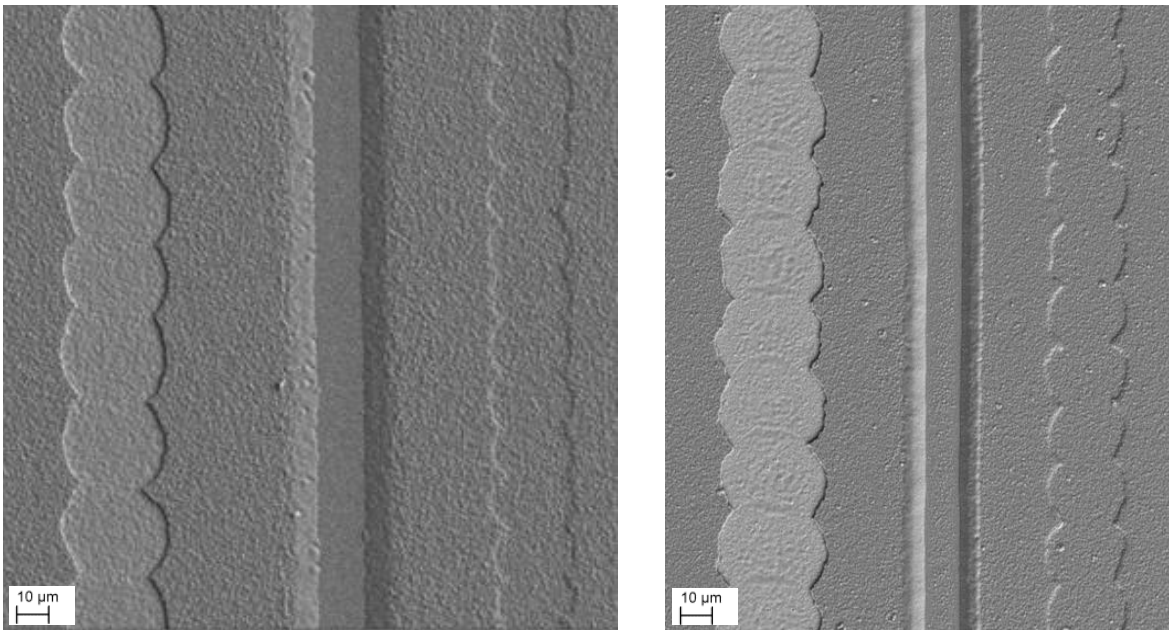

Fig. 8. SEM images of the complete interconnect on finished functional modules. In both images the scribes are arranged in the order P3-P2-P1, from left to right. The area left of P3 and right of P1 is productive cell are, the part in between is non-productive and often called "dead zone". The module depicted on the left was structured using a solid-state laser with 30 ps pulse duration, the module on the right was patterned with a 50 ps all-in-fiber laser system. In both modules the P1 scribe was made at 1064 nm and P2 and P3 scribes were made at 532 nm. The overall width of the dead zone is approximately 155 µm for the left module and 125 µm for the right module.

Electrical characterization was done at Empa, Dübendorf according to section 2.4. Test data is summarized in Tab. 2. All produced modules are working as expected with similar conversion efficiencies. The highest fill factor† is reached on a SSL-scribed module whereas the highest open circuit voltages are found on the fiber-laser structured modules. Four weeks after the initial tests, an anti-reflection coating was applied to the two samples produced with the fiber laser setup.

† The fill factor designates the ratio of the actual maximum obtainable power to the product of the open circuit voltage and short circuit current.

Module ID	Open circuit voltage [V]	Fill factor [%]	Efficiency [%]
SSL_1	4.98	66.2	12.5
SSL_2	4.84	55.2	10.2
FL_1	5.38	63.4	12.5
FL_2	5.38	64.2	12.5

Table 2 Electrical performance data for the functional modules structured with solid-state laser (SSL_1&2) and fiber laser (FL_1&2).

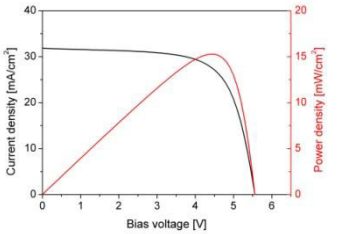

Fig. 9. Illuminated current-voltage (J-V) graph of the best module with 15.3 % efficiency.

In the subsequent second measurement an increase in the fill factor to 67.8 percent and 69.1 percent, respectively and in module efficiency to 14.9 percent and 15.3 percent (designated illumination area) was measured. The illuminated current-voltage curve of the best module is reproduced in Fig. 9. These high module efficiencies are remarkable regarding the fact that the samples were sent by regular post service between labs six times between the process steps.

4. Conclusions and outlook

We have shown the successful implementation of all-laser scribing of CIGS thin-film solar modules on an all-in-fiber 50 ps pulsed MOPA laser system. Validation of the fiber laser as a scribing tool was achieved by adapting and fine-tuning of scribing processes to a 50 ps pulsed all-in-fiber laser. The overall good scribe quality could be maintained also on the new laser platform. A trend was observed for the optimum pulse energy for all processes which is generally higher for the fiber laser. Whether this increase is due to the longer pulse duration or maybe the slightly different pulse shape is subject of ongoing research. With this study we could show that state-of-the art fiber lasers are reliable scribing tools for CIGS thin-film patterning. Due to their form factor and light and compact head they are the most preferable choice for machine-concepts with a fast moving process head. Finally we produced a demonstrator functional module with a dead zone of 125 µm and a module efficiency of 15.3 percent.

Acknowledgements

This work was financed in parts by the Swiss Commission for Technology and Innovation, CTI.

References

Burn, A., Romano, V., Muralt, M., Witte, R., Frei, B., Buecheler, S. and Nishiwaki, S., 2012, "Selective ablation of thin films in latest generation CIGS solar cells with picosecond pulses.", Proc. SPIE 8243, 8243-18, Photonics West 2012.

Chirila, A., Buecheler, S., Pianezzi, F., Bloesch, P., Gretener, C., Uhl, A.R., Fella, C., Kranz, L., Perrenoud, J., Seyrling, S., Verma, R., Nishiwaki, S., Romanyuk, Y.E., Bilger, G. and Tiwari, A.N., 2011, "Highly efficient Cu(In,Ga)Se2 solar cells grown on flexible polymer films" Nature Materials 10, 857-861.

Compaan, A., Matulionis, I. and Nakade, S.,2000,"Laser scribing of polycrystalline thin films.",Optics and Lasers in Engineering, 34, p.15-45.

Gecys, P., Raciukaitis, G., Wehrmann, A., Zimmer, K., Braun, A. and Ragnow, S., 2012, " Scribing of Thin-Film Solar Cells with Picosecond and Femtosecond Lasers", Journal of micro and nanoengineering, Volume: 7 Issue: 1, Pages: 33-37.

Račiukaitis, G., 2011, "Laser Processing by Using Diffractive Optical Laser Beam Shaping Technique.", Journal of Laser Micro/Nano-engineering, 6(1), 37-43.

Witte, R., Frei, B., Schneeberger, S., Buecheler, S. and Nishiwaki, S., Krainer, L., Burn, A., Muralt M. and Romano V., 2013, "Investigation of a reliable all laser scribing process in thin film Cu(In,Ga)(S,Se)2 manufacturing.", Proc. SPIE 8607-47.

Zoppel, S., Huber, H. and Reider, G., 2007, "Selective ablation of thin Mo and TCO films with femtosecond laser pulses for structuring thin film solar cells.", Applied Physics A, 89(1), 161-163.